Rapid Assessment of High RAP Mix with Bio-based Rejuvenators Using Ultrasonic Pulse Velocity and Hamburg Wheel Tracking Testing

Hui Liao
Ph.D. Candidate
University of Waterloo

Aditi Sharma
M.A.Sc. Candidate
University of Waterloo

Pejoohan Tavassoti
Assistant Professor
University of Waterloo

Hassan Baaj
Professor, P. Eng.
University of Waterloo

Paper prepared for presentation at the Innovation in Roadway/Embankment Materials and Geotechnical Engineering of the 2022 TAC Conference & Exhibition, Edmonton, AB

Abstract

Ultrasonic pulse velocity (UPV) is a popular non-destructive testing (NDT) technique for the rapid assessment of materials and infrastructure conditions without causing any damage. UPV is less time-consuming and labour-intensive than conventional inspection techniques commonly applied to the field- and lab-produced asphalt concrete specimens. In this study, different asphalt mix specimens were produced with 50% Reclaimed Asphalt Pavement (RAP) and four bio-based rejuvenators. A control mix with 20% RAP was also prepared with a verified Job Mix Formula (JMF). During the volumetric mix design, the ease of compaction was observed on rejuvenated high RAP mixes in terms of the reduced number of gyrations compared to the control mix. However, the compaction temperature and conditioning time of the high RAP mix was kept the same as the control mix. The volumetric requirements as per Ontario Provincial Standard Specification (OPSS) 1151 were met for the mixes. This paper attempted to use UPV measurements on the rejuvenated high RAP mix and control mix specimens to examine the condition of these mixes, especially those with reduced compaction effort. Different wave characteristics, including group P-wave velocity and peak-to-peak (PTP) amplitude of the first arrival P-wave in the time domain signal, and spectral area, peak spectral magnitudes, peak frequencies in the Fourier spectra, were evaluated to compare the different mixes. After performing UPV tests, the Hamburg Wheel-Track Testing (HWTT) was performed on the same specimens. The results provided a rapid evaluation of the high RAP mixes at high frequency (low temperature) and high temperature (low loading frequency) domains.

Introduction

Ultrasonic pulse velocity (UPV) testing is a well-established non-destructive testing (NDT) technique that has been applied to determine the condition of construction materials such as Portland cement concrete and asphalt concrete. In the UPV testing system, a pulse wave is generated and propagates through the material. And the received signal can be detected to diagnose the material integrity by different wave characteristics (Arabani, Kheiry, & Ferdosi, 2009; Norambuena-Contreras et al., 2010; Tavassoti-Kheiry et al., 2017). When the wave propagates through a specimen, the wave velocity depends on the elastic modulus and density of the medium. Since the compression wave (P-wave) is the fastest wave when transmitting in a solid medium, it is easy to be captured for analysis. Equation (1) shows the relation between the P-wave velocity and modulus of elasticity and density of the material (Jiang, Ponniah, Cascante, & Haas, 2011; Norambuena-Contreras et al., 2010):

$$V_p = \sqrt{\frac{E(1-\nu)}{\rho(1+\nu)(1-2\nu)}} \quad (1)$$

where:

V_p – the group P-wave velocity (m/s)
E – the elastic modulus (Pa).
ρ – the density of the medium (kg/m^3).
ν – Poisson's ratio.

UPV has been applied to asphalt materials to establish the relationship between the ultrasonic characteristics and the mechanical properties of asphalt mixtures. Most research had focused on the wave velocities to compute the elastic modulus of the sample (Medina, Underwood, & Mamlouk, 2018; Tavassoti-Kheiry et al., 2017). Since the UPV test is performed at high frequencies, it is reasonable to expand the reduced frequency range in the master curve by combining the estimated dynamic modulus from the UPV test with the estimated dynamic modulus measured at low-frequency domains. However, due to the heterogeneity of asphalt mix and the non-linear viscous behaviour of asphalt cement (Mounier, Di Benedetto, & Sauzéat, 2012), wave attenuation happens during the wave propagation in asphalt materials. Therefore, other ultrasonic characteristics should also be considered instead of using only wave velocity as an indicator. Jiang et al. (2011) applied different wave characteristics in both time- and frequency-domain signals to establish the correlations with the volumetric properties and dynamic modulus of the asphalt mixes prepared with different gyration numbers. The results showed that the elastic moduli calculated from the P-wave velocity showed a good correlation with gyration number

during compaction due to the consideration of the bulk density (see Equation (1)). Since the increased gyrations resulted in fewer air voids and good bonding between asphalt cement and aggregates, there was less wave attenuation in the specimens with a higher number of gyrations.

Nonetheless, there has been limited research on UPV application on asphalt mixes with high RAP content, especially with the incorporation of rejuvenators. Using a rejuvenator has been proved to be a practical method to allow increased RAP content in Hot Mix Asphalt (HMA). Rejuvenators can soften and reactivate the RAP binder to blend with the virgin materials, thus compensating for the increased stiffness and reduced flexibility due to the aged asphalt cement (Elkashef, Williams, & Cochran, 2018; Mogawer, Fini, Austerman, Booshehrian, & Zada, 2016). One of the conceivable drawbacks of adding rejuvenators is over-softening the mix, especially when with RAP content is above 50%. Due to the overestimated mobilization of the RAP binder, it is possible to have excessive rejuvenator content in the asphalt mix, which will affect the volumetric properties and impair the resistance to permeant deformation (Mogawer, Booshehrian, Vahidi, & Austerman, 2013). The objective of this study was to apply the UPV testing on laboratory mixed and compacted high RAP mix samples with the addition of different bio-based rejuvenators. This paper also evaluated the potential of UPV testing as a rapid assessment tool to reveal the impact of RAP content and rejuvenators on volumetric properties and the rutting performance of asphalt mixes.

Materials and Experimental Plan

Materials

A single source RAP was collected from a local asphalt plant, which has a nominal maximum aggregate size (NMAS) of 12.5mm. Virgin aggregates were provided by the same supplier of RAP. HL3 stone and asphalt sand (AS) fractions from the same quarry were used for mix design, which met the Superpave aggregate consensus property requirements. The NMAS for HL3 and Asphalt Sand were 12.5mm and 4.75mm, respectively. The aggregate gradation results and specific gravities of both virgin aggregates and RAP aggregates are presented in Table 2.

Two virgin asphalt cements that were graded as PG 58-28 and PG 46-34 based on Superpave specifications were selected for this project. PG 58-28 asphalt is commonly used for producing asphalt paving materials in southern Ontario. Whereas the PG 46-34 was not separately used on its own and is chosen in this study as a very soft binder (SB) to counteract the effect of increased RAP content in a new highly recycled HMA mix. The RAP binder was extracted and recovered following the Ontario lab testing manuals, LS 282 – Rev. No.33 (Ministry of Transportation Ontario,

2017) and LS 284 – Rev. No.34 (Ministry of Transportation Ontario, 2020). Table 1 provides the performance grading results of the two virgin binders and recovered RAP binder in accordance with the specifications in AASHTO M320 (2017).

Table 1: Performance grading results of virgin and aged binders

Parameters	Sample Condition	PG 58-28	PG 46-34	RAP Binder
Viscosity @135℃ (Pa·s)	Original	0.267	0.147	1.125
Viscosity @165℃ (Pa·s)		0.083	0.051	0.314
Critical High PG (℃)	Original	60.8	49.7	89.8
	RTFO aged	61.2	49.9	88.6
Critical Intermediate PG (℃)	PAV aged	19.0	10.1	33.1
Critical Low PG (Stiffness) (℃)	PAV aged	-31.8	-36.9	-20.7
Critical Low PG (m-value) (℃)		-31.9	-38.8	-16.8

This study included four commercially available bio-based rejuvenators (Figure 1) that were derived from different sources or produced by different techniques. Respecting suppliers' confidentiality considerations, these rejuvenators were labelled as A, B, D and F to simplify the nomenclature of the rejuvenators in this paper. Figure 1 shows a view of the different rejuvenators used in this study.

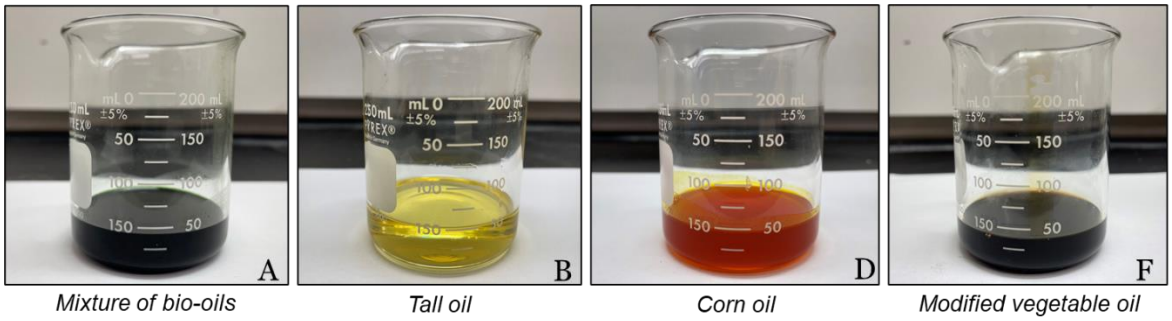

Mixture of bio-oils *Tall oil* *Corn oil* *Modified vegetable oil*

Figure 1: Commercial bio-based rejuvenators

Mix design

The control mix was a Superpave 12.5mm mix with 20% RAP (SP12.5-R20). The job mix formula was provided by the local asphalt plant and has already been used in pavement construction. As for the high RAP mix (SP12.5-R50), the RAP proportion was increased to 50% and the fractions of HL3 and AS were adjusted to maintain a similar gradation to the control mixture. As can be seen in Table 2, the blended gradations of the two mixes are close enough and meet the specification of SP12.5 according to the OPSS 1151 guide (2018).

Table 2: Percent passing (%) of aggregate gradation

Sieve Size (mm)	Aggregate Fractions				Blended Gradation of Mixes		SP12.5 Specification
	HL3	AS	RAP Aggregate		SP12.5-R20	SP12.5-R50	
19	100.0	100.0	100.0		100.0	100.0	
12.5	95.8	100.0	97.8		98.1	97.9	90.0-100.0
9.5	65.4	100.0	87.0		85.4	85.4	28.0-90.0
4.75	4.1	98.1	65.7		59.0	59.9	
2.36	2.5	84.2	53.6		49.9	49.8	28.0-58.0
1.18	1.8	68.8	42.2		40.5	39.8	
0.6	1.4	52.0	31.6		30.7	29.9	
0.3	1.3	29.1	20.3		18.2	18.2	
0.15	1.2	10.1	13.0		8.3	9.5	
0.75	1.0	2.8	8.4		4.0	5.2	2.0-10.0
			Coarse	Fine			
G_{sb}	2.688	2.685	2.685	2.699	2.688	2.690	
G_{sa}	2.795	2.767	2.746	2.785	2.778	2.776	

Table 3 shows the mix design information of the control mix and the high RAP mix with the addition of four abovementioned bio-based rejuvenators. The total asphalt cement content was maintained as 5% for both mix designs. The asphalt cement content of RAP was 4.3%, so the RAP binder replacement for 20% RAP and 50% RAP were 17.1% and 43.0% considering a full blending scenario. The rejuvenator dosage (by weight of the total binder content) of each type of rejuvenator was determined by the binder test results when the rejuvenated binder blend achieved the same critical low PG of the target virgin asphalt cement (PG 58-28). For the mix of SP12.5-R50 with code SB (i.e., soft binder), the added virgin asphalt cement was completely replaced

with PG 46-34 asphalt cement. During the volumetric verification, it was noticed that high RAP mixes needed fewer gyrations to reach the same sample height (115mm), while the volumetric parameters of the high RAP mixes satisfied the SP12.5 mix specifications and achieved similar results to those of the control mix, except the dust to binder ratio.

Table 3: Mix design information

	SP12.5-R20	**SP12.5-R50**				
HL3 (%)	33.2	22.1				
AS (%)	42.7	25.0				
RAP (%)	20.0	50.0				
Added AC (%)	4.1	2.9				
AC (%)	5.0	5.0				
AC RAP (%)	4.3	4.3				
Binder replacement (%)	17.1	43.0				
Rejuvenator code	-	A	B	C	D	SB
Rejuvenator dosage (%)	-	4.03	4.01	4.27	4.52	0
G_{mm}	2.519	2.521	2.526	2.528	2.520	2.518
Design G_{mb}	2.414	-	-	2.419	-	2.415
VMA (%)	14.7	-	-	14.5	-	14.6
VFA (%)	71.5	-	-	72.1	-	72.2
$P_{0.075}/P_{be}$	0.89	-	-	1.16	-	1.15
No. of Gyrations	100	-	-	24	-	25

Sample preparation

The mixing and compaction temperature of an unaged asphalt cement should be determined when the equivalent viscosity values were at 0.17 ± 0.02 Pa·s and 0.28 ± 0.02 Pa·s (Ministry of Transportation Ontario, 2019). Table 4 displayed the mixing and compaction temperatures of two virgin asphalt cements and the blended binders with different rejuvenators.

Table 4: Mixing and compaction temperature (℃)

	PG 58-28	PG 46-34	PG 58-28			
			A	B	D	F
Mixing temp.	146	132	130	132	129	133
Compaction temp.	135	120	115	117	115	120

For the mix with less than 20% RAP, the mixing and compaction temperature remained the same as the unaged virgin asphalt cement (Ministry of Transportation Ontario, 2019). However, due to the limitations of lab mixing equipment, it is difficult to maintain the mixing temperature using a mixing drum without a heating source, especially when a high RAP content is incorporated. It is recommended to increase the mixing temperature and preheat the RAP before mixing for a high RAP mix scenario during the lab mixing procedure (West, Willis, & Marasteanu, 2013). For SP12.5-R50 mixes, the RAP was preheated to 110 (less than 2 hours) before mixing with the virgin aggregates and the mixing temperature was increased to 160℃ to compensate for the increased RAP content and heat loss during the mixing. The sample preparation was completed by following steps:

(1) Preheat aggregates to 10℃ above the mixing temperature overnight (> 16 hrs).
(2) Preheat RAP at 110℃ and maintain the temperature for less than 2 hours before mixing.
(3) Preheat the virgin binder to the mixing temperature and maintain the temperature for less than 1 hour before mixing.
(4) Premix the virgin aggregates with RAP for 45 seconds (30 seconds if %RAP% < 20%), and then add binder to mix another 90 seconds (if %RAP < 20%).
(5) Condition the loose mix for 4 hours at 135℃ to simulate the short-term aging (AASHTO, 2002).
(6) Compact the loose mix using the Superpave Gyratory Compactor (SGC) by controlling the sample height to 63mm.

During the mixing, the temperature of the high RAP loose mix was checked with a thermal gun and a temperature range between 125℃ and 135℃ was achieved before discharging the loose mix. Therefore, this sample preparation procedure was able to attain the mixing temperatures for the binder blends with rejuvenators and the soft binder (see Table 4). Figure 2 shows the compacted samples in this study, two pairs of compacted specimens of each mix type were used to perform the UPV measurements and HWT tests.

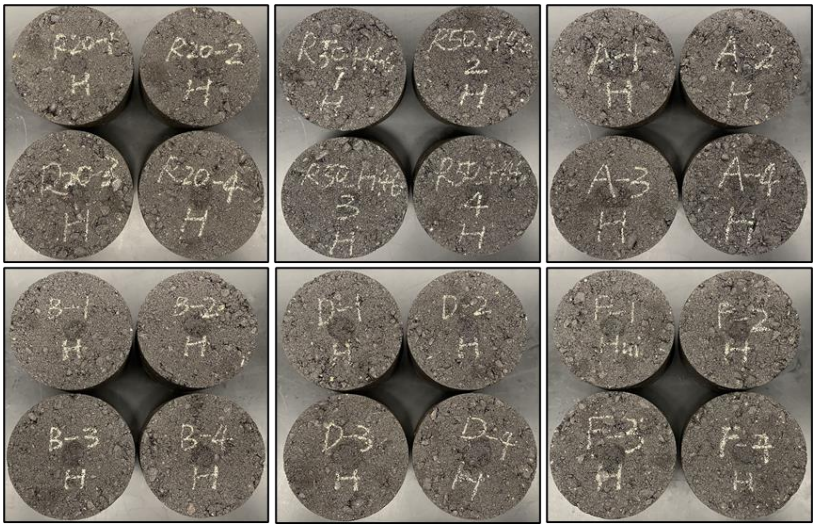

Figure 2: UPV and HWT specimens

Ultrasonic Pulse Velocity (UPV) test

Figure 3 depicts the setup of the UPV measurement system. The devices used in this measurement include a function generator, an oscilloscope, the filter, the piezo driver, and one pair of P-wave transducers (150 kHz) as signal transmitter and receiver. The function generator can generate different types of electrical waveforms over a wide range of frequencies. In this study, a single sine wave pulse with a frequency of 150 kHz was applied to generate the pulse. The output channel of the function generator was connected to a piezo driver which worked as a voltage amplifier to strengthen the input signal. On the receiver transducer side, the received signal was transmitted to the low-pass filter that could pass signals with a frequency lower than a selected cut-off frequency. A 100Hz cut-off frequency was selected, so the signal magnitudes with frequencies lower than 100Hz were essentially zero, which enabled filtering out the noise. The oscilloscope was connected to both the piezo driver and the low-pass filter to capture the real-time input and output signals. The silicone vacuum grease was used as a coupling agent to ensure the contact between the transducer and the surface of the specimen. Also, a piece of sponge was placed beneath the specimen to avoid direct contact with the table, which reduced the disturbance from vibrations and interferences. For each specimen, at least three measurements were performed to verify the repeatability of UPV measurement.

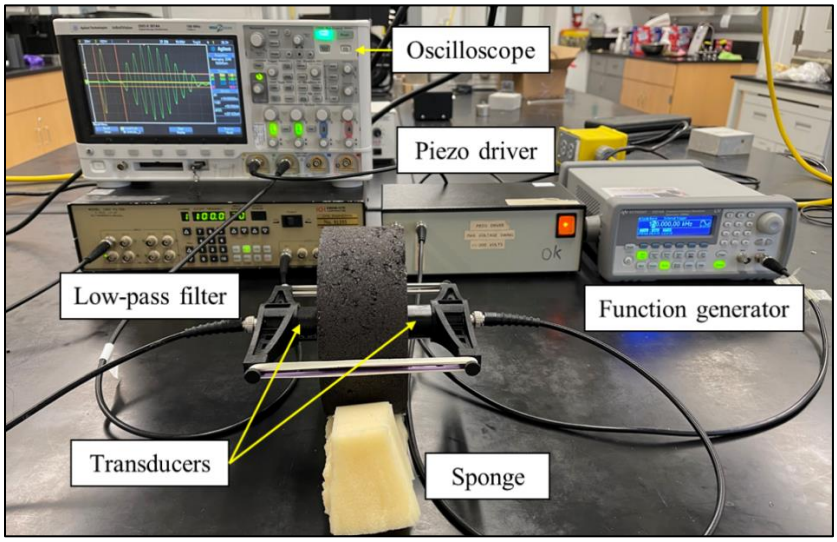

Figure 3: UPV test setup

The wave characteristics determined in this paper were group P-wave velocity, peak-to-peak (PTP) amplitude of the first arrival P-wave in the time domain signal, and maximum spectral magnitudes, spectral area, in the Fourier spectra.

Hamburg wheel-track (HWT) test

After the UPV measurements, the same specimens were used to perform the rutting resistance test. Hamburg wheel-track (HWT) testing is one of the most popular performance tests to evaluate the rutting resistance of asphalt mixture in North America. The HWTT applies the loaded steel wheel directly track the specimens that are submerged in a heated water bath. The load on each side of the wheel is 705 ± 4.5 N. Four specimens with a 150mm diameter are grouped in pairs to run the test at the same time (AASHTO, 2019). The test is programmed to finish when the number of wheel passes reaches 20000 or the rut depth reaches the maximum allowable value, usually 20mm. The rut depth data versus the number of wheel passes will be recorded during the test. Figure 5 showed the HWT device used in this study, a pair of specimens in the mould, and water bath submersion. The water bath temperature is 44℃ for all specimen groups.

Figure 4: HWT devices, sample moulds, and HWT water submersion

Results and Discussion

Volumetric properties

As mentioned above, the number of gyrations of mixes experienced a significant reduction after increasing the RAP content to 50%. As can be seen in Table 5, the average gyration number of the control mix (R20) is 24. While this number decreased to around 15 for the high RAP mixes, except for the mix with rejuvenator F (R0-F), which had an average value of 19. Although the compaction effort varied between different types of mixes, the bulk specific densities (G_{mb}) and air voids (V_a) results exhibited an acceptable coefficient of variation (CV), which proved satisfying repeatability of the sample preparation process. In addition, the air voids of most of the specimens met the requirements (7 ± 0.5%) in the HWT testing standard (AASHTO, 2019). However, the tolerance of target air voids (7%) for the HWT specimens were suggested to be raised to 1% or even 2% in some DOT specification in North America. Regarding this adjustment, the measured air voids of all the specimens were within the 1% deviation of 7%. For each specimen group, the correlation between the number of gyrations and $\mathrm{G_{mb}}$ (or air voids) was calculated, and the values were all above 0.93, which indicated a positive relationship between the number of gyrations and the specimen density.

Table 5: Volumetric properties of mix specimens

Specimens		Parameters			Specimens		Parameters		
		Gyr.	G_{mb}	V_a			Gyr.	G_{mb}	V_a
	1	23	2.341	7.08%		1	13	2.347	7.08%
	2	22	2.341	7.08%		2	16	2.367	6.29%
	3	34	2.347	6.82%		3	14	2.351	6.93%
R20	4	18	2.335	7.31%	R50-B	4	15	2.357	6.69%
	Mean	***24.3***	***2.341***	***7.07%***		Mean	***14.5***	***2.355***	***6.75%***
	Std.	***6.8***	***0.005***	***0.20%***		Std.	***1.3***	***0.009***	***0.35%***
	CV (%)	***28.2***	***0.2***	***2.8***		CV (%)	***8.9***	***0.4***	***5.1***
	1	16	2.351	6.60%		1	16	2.358	6.72%
	2	14	2.345	6.87%		2	14	2.349	7.10%
	3	13	2.343	6.95%		3	12	2.344	7.28%
R50-SB	4	14	2.346	6.81%	R50-D	4	16	2.362	6.58%
	Mean	***14.3***	***2.346***	***6.81%***		Mean	***14.5***	***2.353***	***6.92%***
	Std.	***1.3***	***0.004***	***0.15%***		Std.	***1.9***	***0.008***	***0.33%***
	CV (%)	***8.8***	***0.2***	***2.2***		CV (%)	***13.2***	***0.4***	***4.7***
	1	18	2.366	6.17%		1	16	2.351	6.72%
	2	17	2.360	6.39%		2	23	2.360	6.35%
	3	13	2.351	6.78%		3	15	2.344	6.97%
R50-A	4	17	2.369	6.03%	R50-F	4	20	2.353	6.63%
	Mean	***16.3***	***2.362***	***6.34%***		Mean	***18.5***	***2.352***	***6.67%***
	Std.	***2.2***	***0.008***	***0.32%***		Std.	***3.7***	***0.006***	***0.25%***
	CV (%)	***13.6***	***0.3***	***5.1***		CV (%)	***20.0***	***0.3***	***3.8***

The incorporation of a high amount of RAP will increase the air voids and reduce the mix workability due to the stiff aged asphalt cement, whereas the addition of a rejuvenator or soft binder appeared to mitigate the increase in air voids. This observation is also in line with findings from the past research (Mogawer et al., 2013). In this study, the rejuvenator dosage was determined based on the binder blending test results, which represented a full blending scenario between the RAP binder and the blend of virgin asphalt cement with a rejuvenator. However, the full blending case was unlikely to happen during the mixing stage, leading to less binder contribution from RAP immediately after mixing. Due to the insufficient diffusion between the rejuvenator and RAP, it is expected that there will be excess free rejuvenator in the loose mix. The extra lubricating effect resulting from the free rejuvenator potentially contributed to the ease

of compaction observed in this study. Nevertheless, the volumetric requirements were successfully achieved, and no adverse effect was observed in terms of mix tenderness.

Wave characteristics

Figure 5 showed the input and output time signals captured during the UPV measurement. Since the signal strength was affected by the amount of coupling agent and the loading force induced by the transducer holders, the output time signal was normalized using MATLAB normalize function before performing the Fourier transformation. The travel time of the P-wave can be calculated by subtracting the starting time of the input signal by the arrival time of the first wave in the output signal. The wave velocity was then determined by dividing the distance (sample height) between the two transducers by the time of flight. As shown in Table 6, the calculated group velocity was around 3300m/s, so the wavelength (λ) of the signal could be estimated using the group velocity and the transducer frequency (150kHz). The wavelength was used to verify the selection of frequency of the transducers. When the maximum aggregate size of the specimen is larger than the wavelength, wave attenuation increases due to excessive scattering (Abo-Qudais & Suleiman, 2005). Also, the ratio between the wave travel distance (i.e., specimen length, L) and the wavelength should be greater than three to reduce the near field effects (Jiang et al., 2011). In this paper, $\lambda \approx 22mm > 12.5mm$ and $L/\lambda = 63mm/22mm \approx 2.86$. Due to the availability of transducers, the 150kHz transducers were the best applicable in this UPV testing. To remove the interference with other waves, such as shear wave and Rayleigh wave, a modified cosine function window was applied to separate the first P-wave (see Figure 5).

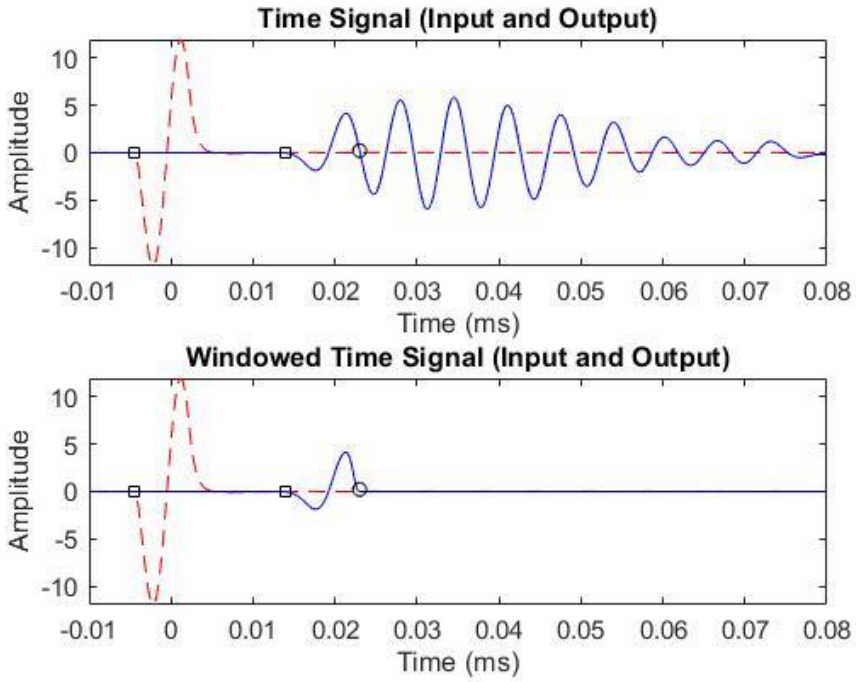

Figure 5: Time signals before and after windowing

The Fourier transformation of the first arrival P-wave was accomplished in MATLAB using the Fast Fourier Transform (FFT) function, the frequency components after 400kHz were not included as the wavelength was in the order of the aggregate size.

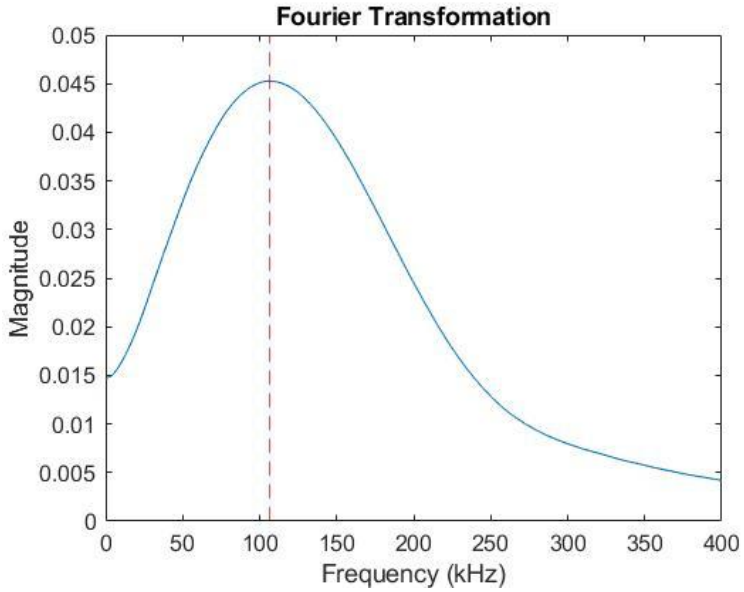

Figure 6: Fourier transformation of the windowed time signal

Table 6 showed the parameters obtained from both the time signals and frequency domain spectra. The result was averaged by the four replicate specimens for each mix type. The Poisson's ratio of the specimen was assumed 0.28 at room temperature for calculating the elastic modulus (Tavassoti-Kheiry et al., 2017). The corresponding coefficients of variation of each mix type were also presented in Table 7. Generally, wave parameters such as group velocity, elastic modulus, spectral area, and dominant frequency showed relatively higher repeatability, while the rest parameters also achieved acceptable coefficient of variations (< 16%). However, the differences in group velocity and computed elastic modulus between different mixes were negligible. As for the parameters derived from the Fourier spectra, the dominant frequencies of the rejuvenated high RAP mixes were 2 to 3 kHz higher than that of the control mix. The spectral area and max magnitude results shown in Table 6 were not significantly different between the control mix and the rejuvenated high RAP mixes, except for R50-F.

Table 6: Wave parameters of different mixes

Mix	Velocity (m/s)	Elastic modulus (MPa)	PTP amplitude	Dominant freq. (kHz)	Max magnitude	Spectral area
R-20	3324.12	20246.81	4.79	109.94	0.035	15.43
R50-SB	3315.77	20187.46	5.16	112.95	0.037	17.00
R50-A	3399.29	21349.92	4.82	112.90	0.034	15.77
R50-B	3342.20	20584.66	5.08	112.78	0.036	16.33
R50-D	3321.17	20308.10	5.04	111.95	0.036	16.60
R50-F	3279.42	19790.76	4.09	111.61	0.029	13.84

Table 7: Coefficient of variation (%) of different parameters

Mix	Velocity (m/s)	Elastic modulus (MPa)	PTP amplitude	Dominant freq. (kHz)	Max magnitude	Spectral area
R-20	2.9	5.8	5.5	2.1	4.8	4.4
R50-SB	2.5	5.0	12.7	4.6	15.8	12.9
R50-A	1.4	3.2	10.1	3.6	10.7	11.4
R50-B	1.4	3.0	12.1	2.5	14.4	11.2
R50-D	1.7	3.6	13.7	3.1	15.4	13.5
R50-F	2.2	4.4	11.7	4.4	15.8	13.3

The marginal variations in the wave parameters observed in this paper were different from the work conducted by Jiang et al. (2011), in which the wave characteristics obtained from the Fourier spectra showed a good correlation with the gyration number, density, and dynamic modulus of the mixes. Although the mixes were prepared with different numbers of gyrations, the specimen heights were also different regarding the varied compaction effort. In contrast, the specimens prepared in this paper had similar gradation and binder content and were compacted to the same sample heights. Therefore, the wave characteristics are more sensitive to the length and physical properties, such as density and air voids, of the compacted asphalt mix sample. The UPV testing primarily provides bulk properties of the medium, and hence was not capable of distinguishing the specimen changes if the asphalt mix specimens had the same geometric and volumetric properties, even though the binder properties were different. However, the similarity of the wave parameter results indicated there were no internal defects inside the specimens or a significant lack of binding between materials, which excluded the concerns of reduced compaction effort on rejuvenated high RAP mix samples. Nevertheless, this technique can be effectively used to rapidly assess the compacted specimens in terms of consistency and provide a relative comparison of the engineering properties in terms of the modulus values.

Rutting performance

Figure 7 illustrates the rut depth evolution of the different mixes against the load wheel passes. The control mix (R20) exhibited the best rutting resistance in terms of the smallest rut depth (8.9mm) after 20000 passes. The high RAP mixes showed increased rut depth compared to the control mix. Based on the results of HWT tests screening, mixes of R50-D and R50-F were eliminated as they reached the maximum allowable deformation much earlier than 20000 passes. However, the high RAP mixes with rejuvenators A and B, and the soft binder showed an acceptable performance while a slight increase (1 to 2 mm) of the maximum rut depth could be noticed as compared to the R20. The stripping inflection point of these mixes occurred earlier than that of the control mix. This emphasizes that solely relying on binder studies to find the optimized dosage would not be enough to yield acceptable mix performance. To this end, two major aspects should be considered: 1) adjusting the rejuvenator content proportional to the mix production practices (e.g., availability of silo storage to help with diffusion and blending of rejuvenator and aged binder, or desirable level of ease of compaction in construction without sacrificing the constructability); and 2) utilizing performance evaluation methods on the mix level to better screen the effectiveness of rejuvenators, especially in case of high-RAP contents.

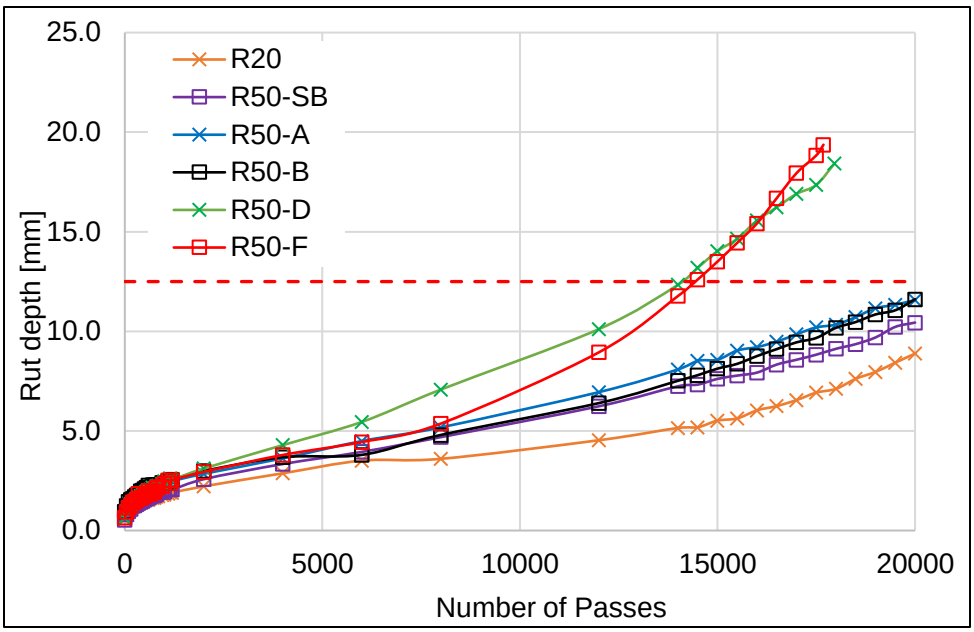

Figure 7: Rut depth versus wheel passes

In the early stage of HWT testing, the sample will continue to consolidate for the first few numbers of passes. It represents the densification of the asphalt mix caused by vehicle loading when the compacted pavement is open to traffic. The rut depth measured before 1000 passes can be attributed to the post-compaction consolidation. Figure 8 shows the rut depth of the mix specimens after 1000 passes. The control mix samples showed relatively smaller rut depth than those of the high RAP mixes with rejuvenators. However, the high RAP mix specimens prepared with the soft binder only showed a marginal increase in the deformation compared to the control mix. The results indicated that the mixes with a smaller number of gyrations would have more post-compaction condensation during the rutting test.

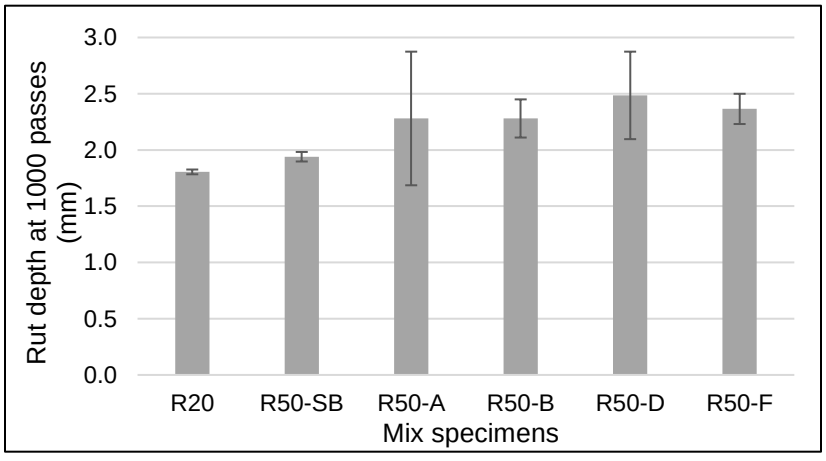

Figure 8: Rut depth at 1000 passes

Conclusions

This paper attempted rapid assessment of asphalt mixes with different RAP contents and bio-based rejuvenators. To this end, Ultrasonic Pulse Velocity (UPV) measurements and Hamburg Wheel Tracking (HWT) tests were employed to study the compacted asphalt mixes. The following conclusions can be drawn based on the volumetric properties, wave parameters, and rutting test results:

1. The ease of compaction observed during the specimen preparation can be attributed to the extra lubricating effect due to the presence of excessive rejuvenator content. The rejuvenator dosage might need adjustment based on the contribution of the activated RAP binder, rather than solely relying on optimization at the binder scale.
2. The wave parameters obtained in both the time domain and the frequency domain were repeatable within the same mix specimen group. However, the results of those parameters were not significantly different between mix types.
3. The similarity of the wave parameters between different mixes, achieving the same level of high-frequency modulus among the mixes can be used as a tool for assessing consistency of samples production and presence of a major internal defect in the mixes.
4. HWT testing can be effectively used as a screening tool to distinguish different rejuvenators and high RAP mixes in terms of their rutting resistance and moisture damage performance in the design stage.
5. Preliminary results from HWT tests suggest that mixes with a lower number of gyrations showed greater post-compaction condensation depth in the early stage of the rutting test.

Acknowledgements

We acknowledge the support of the Natural Sciences and Engineering Research Council of Canada (NSERC). We also acknowledge the support of our industry partners, Imperial Oil Ltd., and Steed & Evans Ltd., for their contribution to the project. We would like to thank the Non-destructive test (NDT) lab in University of Waterloo for providing the test equipment.

References

AASHTO. (2002). *Standard Practice for Mixture Conditioning of Hot Mix Asphalt (HMA)*. AASTHO R 30-02 (2019), Washington D.C.: American Association of State Highway and Transportation Officials.

AASHTO. (2017). *Standard Specification for Performance-Graded Asphalt Binder*. AASHTO M 320-17, Washington D.C.: American Association of State Highway and Transportation Officials.

AASHTO. (2019). *Standard method of test for Hamburg wheel-track testing of compacted asphalt mixtures*. AASTHO T 324, Washington D.C.: American Association of State Highway and Transportation Officials.

Abo-Qudais, S., & Suleiman, A. (2005). Monitoring fatigue famage and crack healing by ultrasound wave velocity. *Nondestructive Testing and Evaluation*, *20*(2), 125–145. https://doi.org/10.1080/10589750500206774

Arabani, M., Kheiry, P. T., & Ferdosi, B. (2009). Laboratory evaluation of the effect of hma mixt parameters on ultrasonic pulse wave velocities. *Road Materials and Pavement Design*, *10*(1), 223–232. https://doi.org/10.1080/14680629.2009.9690189

Elkashef, M., Williams, R. C., & Cochran, E. (2018). Investigation of fatigue and thermal cracking behavior of rejuvenated reclaimed asphalt pavement binders and mixtures. *International Journal of Fatigue*, *108*, 90–95. https://doi.org/10.1016/j.ijfatigue.2017.11.013

Jiang, Z., Ponniah, J., Cascante, G., & Haas, R. (2011). Nondestructive ultrasonic testing methodology for condition assessment of hot mix asphalt specimens. *Canadian Journal of Civil Engineering*, *38*(7), 751–761. https://doi.org/10.1139/L11-046

Medina, J. R., Underwood, B. S., & Mamlouk, M. (2018). Estimation of Asphalt Concrete Modulus Using the Ultrasonic Pulse Velocity Test. *Journal of Transportation Engineering, Part B: Pavements*, *144*(2), 04018008. https://doi.org/10.1061/jpeodx.0000036

Ministry of Transportation Ontario. (2017). *Method of Test for Quantitative Extraction of Asphalt Cement and Analysis of Extracted Aggregate*.

Ministry of Transportation Ontario. (2018). *Material Specification for Hot Mix Asphalt (OPSS.MUNI 1150)* (pp. 1–20). pp. 1–20. Ontario, Canada.

Ministry of Transportation Ontario. (2019). *Design Procedure for Recycled Hot Mix Asphalt*.

Ministry of Transportation Ontario. (2020). *Method of Test for Recovery of Asphalt From Solution By Rotary Evaporator*.

Mogawer, W. S., Booshehrian, A., Vahidi, S., & Austerman, A. J. (2013). Evaluating the effect of rejuvenators on the degree of blending and performance of high RAP, RAS, and RAP/RAS mixtures. *Road Materials and Pavement Design*, *14*, 193–213. https://doi.org/10.1080/14680629.2013.812836

Mogawer, W. S., Fini, E. H., Austerman, A. J., Booshehrian, A., & Zada, B. (2016). Performance characteristics of high reclaimed asphalt pavement containing bio-modifier. *Road Materials and Pavement Design*, *17*(3), 753–767. https://doi.org/10.1080/14680629.2015.1096820

Mounier, D., Di Benedetto, H., & Sauzéat, C. (2012). Determination of bituminous mixtures linear properties using ultrasonic wave propagation. *Construction and Building Materials*, *36*, 638–647. https://doi.org/10.1016/j.conbuildmat.2012.04.136

Norambuena-Contreras, J., Castro-Fresno, D., Vega-Zamanillo, A., Celaya, M., & Lombillo-Vozmediano, I. (2010). Dynamic modulus of asphalt mixture by ultrasonic direct test. *NDT and E International*, *43*(7), 629–634. https://doi.org/10.1016/j.ndteint.2010.06.007

Tavassoti-Kheiry, P., Boz, I., Chen, X., & Solaimanian, M. (2017). Application of Ultrasonic Pulse Velocity Testing of Asphalt Concrete Mixtures to Improve the Prediction Accuracy of Dynamic Modulus Master Curve. *Airfield and Highway Pavements 2017: Testing and Characterization*

of Bound and Unbound Pavement Materials - Proceedings of the International Conference on Highway Pavements and Airfield Technology 2017, *2017-Augus*, 152–164. https://doi.org/10.1061/9780784480939.014

West, R., Willis, J. R., & Marasteanu, M. (2013). Improved Mix Design, Evaluation, and Materials Management Practices for Hot Mix Asphalt with High Reclaimed Asphalt Pavement Content. In *National Cooperative Highway Research Program*. https://doi.org/10.17226/22554